Production of peroxy nitrates in boreal biomass burning plumes over Canada during the BORTAS campaign

Marcella Busilacchio[1], Piero Di Carlo[1,2], Eleonora Aruffo[1,2], Fabio Biancofiore[1,2], Cesare Dari Salisburgo[1], Franco Giammaria[2], Stephane Bauguitte[3], James Lee[4], Sarah Moller[4], James Hopkins[4], Shalini Punjabi[4], Stephen Andrews[4], Alistair C. Lewis[4], Mark Parrington[5,*], Paul I. Palmer[5], Edward Hyer[6], Glenn M. Wolfe[7,8]

[1] Center of Excellence CETEMPS, Universita' dell'Aquila, Via Vetoio, Coppito, L'Aquila, Italy,

[2] Department of Physical and Chemical Sciences, University of L'Aquila, Coppito L'Aquila, Italy,

[3] Facility for Airborne Atmospheric Measurements, Bedfordshire, UK,

[4] Department of Chemistry, University of York, York, UK,

[5] School of GeoSciences, University of Edinburgh, UK.

[6] Marine Meteorology Division, Naval Research Laboratory, Monterey, California, USA.

[7] Atmospheric Chemistry and Dynamics Laboratory, NASA Goddard Space Flight Center, Greenbelt, Maryland, USA

[8] Joint Center for Earth Systems Technology, University of Maryland Baltimore County, Baltimore, MD, USA

[*] now at European Centre for Medium-Range Weather Forecasts (ECMWF), Reading, UK.

Correspondence to: P. Di Carlo (piero.dicarlo@aquila.infn.it)

Abstract

The observations collected during the BORTAS campaign in summer 2011 over Canada are analysed to study the impact of forest fire emissions on the formation of ozone (O_3) and total peroxy nitrates ($\sum$PNs, $\sum ROONO_2$). The suite of measurements onboard the BAe-146 aircraft, deployed in this campaign, allows us to calculate the production of O_3 and of ΣPNs, a long lived

NO_x reservoir whose concentration is supposed to be impacted by biomass burning emissions. In fire plumes, profiles of carbon monoxide (CO), which is a well-established tracer of pyrogenic emission, show concentration enhancements that are in strong correspondence with a significant increase of ΣPNs concentrations, whereas minimal increase of the concentrations of O_3 and NO_2 are observed. The ΣPNs and O_3 productions have been calculated using the rate constants of the first and second order reactions of Volatile Organic Compounds (VOCs) oxidation. The ΣPNs and O_3 productions have also been quantified by 0-D model simulation based on the Master Chemical Mechanism. Both methods show that in fire plumes the average production of ΣPNs and O_3 are greater than in the background plumes, but the increase of ΣPNs production is more pronounced than the O_3 production. The average ΣPNs production in fires plumes is from 7 to 12 times greater than in the background, whereas the average O_3 production in fires plumes is from 2 to 5 times greater than in the background. These results suggest that, at least for boreal forest fires and for the measurements recorded during the BORTAS campaign, fire emissions impact both the oxidized NO_y and O_3, but: 1) ΣPNs production is amplified significantly more than O_3 production and 2) in the forest fire plumes the ratio between the O_3 production and the ΣPNs production is lower than the ratio evaluated in the background air masses, thus confirming that the role played by the ΣPNs produced during biomass burning is significant in the O_3 budget. These observations are consistent with elevated production of PAN and concurrent low production (or sometimes loss) of O_3 observed in some another campaigns (i.e. ARCTAS-B) focused on forest fire emissions. Moreover our observations extend ARCTAS-B results since PAN is one of the compounds included in the ΣPNs family detected during BORTAS. The implication of these observations is that fire emissions in some cases, for example Boreal forest fires and in the conditions reported here, may influence more long lived precursors of O_3 than short lived pollutants, which in turn can be transported and eventually diluted in a wide area. These observations provide additional indirect evidence that O_3 production may be enhanced as plumes from forest fires age.

1. Introduction

Biomass burning emissions are an important atmospheric source of fine carbonaceous particles, trace gases and aerosols that significantly affect the chemical composition of the atmosphere and the radiation balance of the Earth-atmosphere system (Crutzen et al., 1979; Crutzen and Andreae, 1990; Andreae and Merlet, 2001; Bond et al., 2004; Langmann et al., 2009; Bowman et al., 2009). Biomass burning generates large quantities of carbon monoxide (CO), nitrogen oxides (NO_x= NO+NO_2) and VOCs which are the major precursors involved in the photochemical production of tropospheric ozone (O_3) (Goode et al., 2000, Chan et al., 2003). Moreover, biomass burning emissions include some greenhouse gases (CO_2, CH_4, N_2O) that alter the climate and air quality (Langmann et al., 2009; Lapina et al., 2006; Simpson et al., 2006). Quantification of the influence of boreal forest fires on the Earth-atmosphere system and on the climate has become one of the key topics for the scientific community.

Forest fires in the boreal regions of Siberia, Canada and Alaska peak during the period from May to October (Lavoue et al., 2000). Some studies highlight the increase in the number of boreal forest fires and the total forested area burned over Canada during the past three decades, corresponding to increasing temperatures and reduced moisture in this area (Gillett et al., 2004; Rinsland 2007; Marlon 2008). Wotton et al. (2010) estimate an increase of 30% in boreal forest fire occurrence by 2030, causing a possible growth of 30% in the emission of CO_2 and other greenhouse gases (Amiro et al., 2009). The effects of boreal biomass burning emissions on the O_3 concentration has been investigated by several authors with some studies showing situations where O_3 concentrations increase and others where it was unaffected (e.g., Wofsy et al., 1992; Jacob et al., 1992; Mauzerall et al., 1996;Wotawa and Trainer, 2000; Val Martin et al., 2006; Real et al., 2007; Leung et al., 2007, Jaffe and Wigder,2012, Parrington et al., 2012). The analysis of the ARCTAS-B (NASA Arctic Research of the Composition of the Troposphere from Aircraft and Satellites) aircraft measurements of biomass burning plumes in central Canada in the spring and summer of 2008 showed consistent production of peroxyacetyl nitrate (PAN), with little evidence for O_3 formation and, in some

plumes, the O_3 mixing ratios measured within boreal biomass burning plumes were indistinguishable from measurements outside of the plumes (Alvarado et al., 2010). The production of ozone $P(O_3)$ measured in boreal fire plumes has been reported to be a function of the plume age (Parrington et al., 2013), but with mixed, non-conclusive results. For example, boreal fire plumes transported over the Azores and measured between 1 and 2 weeks after emission showed an O_3 increase between 40% and 90% (Val Martin et al., 2006; Pfister et al., 2006). On the other hand, observations over Siberia in 2006 of aged boreal fire plumes (up to a week) showed some plumes with O_3 enhanced and others with O_3 depletion; on average, the O_3 in the fire plumes was not significantly different from that in the background atmosphere (Verma et al., 2009). In earlier studies of relatively fresh plumes (1-2 days), O_3 was reported to be enhanced in one third of the boreal fire plumes with concentrations in the remaining plumes being unaffected (Wofsy et al. 1992; Mauzerall et al. 1996).

In the atmosphere, volatile organic compounds (VOCs) are oxidized by OH, NO_3 or O_3 producing an alkyl radical R that rapidly reacts with molecular oxygen O_2 to form peroxy radicals (HO_2, RO_2) (reaction R1). The RO_2, then, can proceed in different ways: 1) reacting with NO and producing a molecule of alkyl nitrate (ΣANs, $\sum RONO_2$) (R2) or an alkoxy radical RO (R4) or 2) reacting with NO_2 and producing peroxy nitrates (ΣPNs, $\sum ROONO_2$) (R3). Reactions (R4) and (R3) have opposite effects on the O_3 budget, propagating or terminating radical cycles, respectively. Thus, peroxy nitrate formation competes with the O_3 production resulting from reactions (R4)-(R8). Alkyl nitrate formation via (R2) can also affect the O_3 budget. The reaction cycles that are of interest when considering Nitrogen oxides (NO_x) and odd-hydrogen radicals (HO_x) (R1-R8) are illustrated schematically in Figure 1 and listed below:

$$OH + RH + O_2 + M \rightarrow RO_2 + H_2O + M \quad \text{(R1)}$$

$$RO_2 + NO + M \rightarrow RONO_2 + M \quad \text{(R2)}$$

$$RO_2 + NO_2 + M \rightarrow RO_2NO_2 + M \quad \text{(R3)}$$

$$RO_2 + NO \rightarrow RO + NO_2 \quad \text{(R4)}$$

$$RO + O_2 \rightarrow R'C(O)R'' + HO_2 \quad \text{(R5)}$$

$$HO_2 + NO \rightarrow OH + NO_2 \quad \text{(R6)}$$

$$NO_2 + h\nu \rightarrow NO + O \quad \text{(R7)}$$

$$O + O_2 + M \rightarrow O_3 + M \quad \text{(R8)}$$

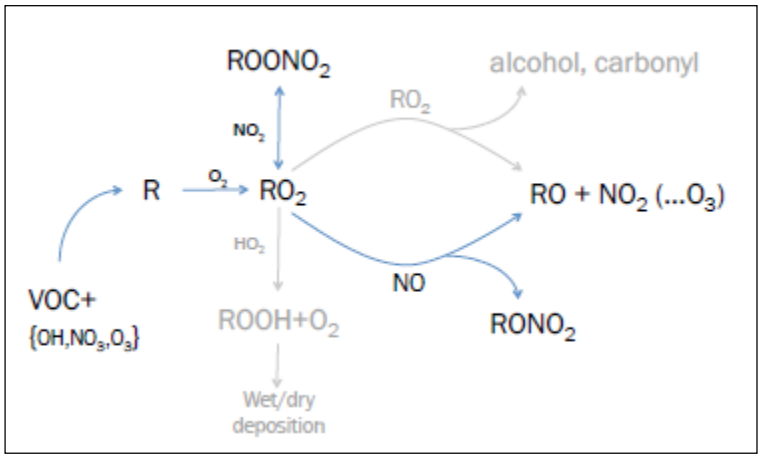

Figure 1. A schematic of the atmospheric chemical system (Atkinson and Arey, 2003, Palmer et al.2013).

In July and August 2011, the BOReal forest fires on Tropospheric oxidants over the Atlantic using Aircraft and Satellites (BORTAS) measurement campaign was carried out in order to quantify the impact of boreal biomass burning on the composition and distribution of tropospheric oxidants. The BORTAS project involved several international institutions with the support of the UK Facility for Airborne Atmospheric Measurements (FAAM). The instruments were installed on board the FAAM BAe146 research aircraft and the campaign was based at Halifax airport (Nova Scotia, Canada). During the campaign, fifteen flights were carried out (nominally referenced as flights B618 to B632) in Eastern Canada that were planned to maximize the probability of sampling air masses produced from forest fires in Canada (Ontario) or the USA. More detailed information about the

BORTAS campaign objectives and preliminary results are presented by Palmer et al. (2013). The primary aim of this study is to evaluate and understand the impact of the boreal fire emissions during the BORTAS campaign on the formation of O_3 and ΣPNs within biomass burning plumes and, in particular, to estimate the balance between the production of ozone $P(O_3)$ and the production of total peroxy nitrates $P(\Sigma PNs)$ in this specific environment.

2. Instrumental

A comprehensive description of the BORTAS experiment and of the overall instrumentations involved can be found in Palmer et al. (2013). Measurements included in this analysis are summarized in Table 1. NO_2, ΣPNs and ΣANs were measured using the TD-LIF (Thermal Dissociation – Laser Induced Fluorescence) instrument developed at the University of L'Aquila (Italy) (Dari-Salisburgo et al., 2009; Di Carlo et al., 2013). Briefly, this technique permits direct measurement of NO_2 molecules excited by laser radiation. The ΣPNs and ΣANs are measured after thermal-dissociation into NO_2 by heating the air sample at 200°C and 400°C, respectively (Day et al., 2002; Di Carlo et al., 2013). Nault et al. (2015) found that methyl peroxy nitrate ($CH_3O_2NO_2$), which can be abundant in particular conditions (very low temperature, below 240K, typical of the high atmosphere), may contribute interference to high altitude NO_2 measurements resulting from thermal decomposition occurring in the sample intake system. This interference is a function of the intake system temperature and increases from 280 K in which the interference is negligible up to 300 K in which it can be on the order of 10%. During all the BORTAS flights analysed in this paper, the cabin temperature has been kept at about 280 K and, as a consequence, the impact on the NO_2 of the $CH_3O_2NO_2$ dissociation is negligible. Moreover, this species is not expected to be significant in our study, since the ambient temperatures of the air masses sampled during the period in analysis range between 250 K and 280 K and the $CH_3O_2NO_2$ concentration is significant only for temperatures lower than 240 K. The measurements of O_3 were carried out with an UV absorption

system Model 49C (Thermo environmental Corp.) (Wilson and Birks, 2006). CO was measured using a VUV resonance/fluorescence system (Gerbig et al. (1999). A chemiluminescence instrument equipped with a photolytic converter was also used to measure NO and NO_2 (Lee et al. 2009; Reidmiller et al. 2010). VOC concentrations were measured by the University of York using a WAS (Whole Air Sampling) system coupled to an offline GC-FID (Gas Chromatography with Flame Ionization Detector) (Hopkins et al. 2003; Purvis et al. 2013) and by the University of East Anglia using a PTR-MS (Murphy et al. 2010).

Table 1. Observed compounds and instruments on board the BAe-146 aircraft during BORTAS campaign, used in the analysis in this paper. A complete list of the instruments with accuracy and detection limit, is reported in Palmer et al. (2013).

Species	**Method**	**Reference**
CO	VUV resonance/fluorescence	Gerbig et al. (1999)
O_3	UV absorption	Wilson and Birks (2006)
NO_2 , ΣRO_2NO_2, $\Sigma RONO2$, NO_y	TD-LIF	Dari-Salisburgo et al. (2008); Di Carlo et al. (2013)
C_5–C_{12} VOCs	GC-MS	Purvis et al. (2013)
C_2–C_7 NMHCs, acetone CH_3OH	WAS-GC-FID	Hopkins et al. (2003)
CH_3CN, C_3H_6O, C_5H_8, MVK+MACR, C_4H_8O, C_6H_6, C_7H_8, $C_{10}H_{16}$	PTR-MS	Murphy et al. (2010)

3. Data analysis

3.1 Geographical location and meteorological situation

Fig. 2 shows the geographic coverage of the five flights selected for our analysis. The flights were carried out between 12th July and 3rd August 2011 over Canada and, in particular, above the North

Atlantic Ocean, Nova Scotia, Maine and Québec. The altitude during the flights exceeded a typical planetary boundary layer depth of 2000 m a.s.l. so that local emissions do not affect the measurements, especially those carried out in the fire plumes. Table 2 summarizes some specific features of each flight BORTAS selected in this analysis and provides a brief description of the meteorology associated with them. Other details about the BORTAS flights can be found in Palmer et al. (2013). From these descriptions, it can be seen that the synoptic situation of the fire plume flights are similar to those of background flights.

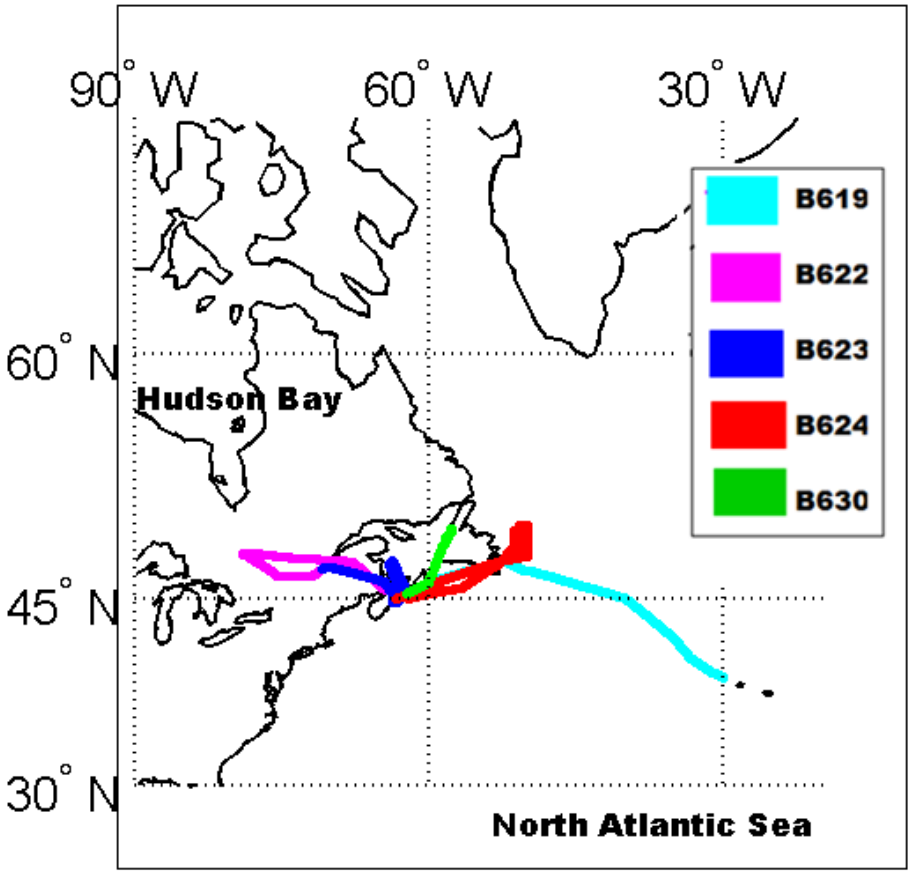

Figure 2. FAAM146 flight tracks during July 2011. The different colours are the tracks of each different flight: during the B623 and B624 fire plumes were observed, during B619 and B630

1 background air was measured, whereas in the B622 flight fire plume and background air were
2 detected. See Table 2 for details of individual flights
3

Table 2. Synoptic meteorology and weather associated with the five BORTAS flights considered in this analysis.

Flight	Date	Trajectory	Flight Altitude (Max-Min-Mean)	Synoptic meteorology
B619 (background)	13/07/2011	St John's-Halifax	7257 100 4594	Skies mostly cloudy.
B622 (fire plume and background)	20/07/2011	Halifax – Québec City	7575 1892 4699	Low from surface to 500 hPa S Ungava Bay. Surface low and frontal wave moving E from mouth of St Lawrence. Flight in "warm" sector – Mainly clear to 21:00 then cloudy.
B623 (fire plume)	20/07/2011	Québec City–Halifax	6173 1888 4451	Low from surface to 500 hPa S Ungava Bay. Surface low and frontal wave just N of Anticosti Island and cold front west. Showers and thundershowers along and in advance of front. Aircraft may have encountered showers over Prince Edward Island (PEI).
B624 (fire plume)	21/07/2011	Halifax - St John's – Halifax	2826 1743 2069	Low from surface to 500 hPa over extreme N Labrador. Cold front from NB to S of NF (Newfoundland). Weak low crossing NB late day. Cloud moved into flight zone from the west. Precipitation for return flight from S of NF to Halifax.
B630 (background)	31/07/2011	Halifax, Nova Scotia	7616 5076 6704	Trough from surface through to 500 hPa along Labrador coast to low centre off south coast NF. Cooler air mass over region. Weak ridge building over NB to W Labrador. Generally clear skies for flight route and level.

3.2 Identification of the plumes: vertical profiles and back trajectories

CO is a product of incomplete combustion (Crutzen et al., 1979; Andreae and Merlet, 2001; Lewis et al., 2013), therefore it is one of the tracers used to classify the plumes emitted by boreal fires. However, it is necessary to discriminate between anthropogenic and biomass burning CO emissions; for this purpose, following Lewis et al. (2013), we defined a CO threshold of 200 ppbv and we verified at the same time the presence of other pyrogenics such as furfural or camphor to confirm the fire origin of the plume. In conclusion, we classify the air masses in three classes: 1) those sampled within boreal biomass burning plumes ($CO \geq 200$ ppbv with significant presence of other pyrogenics species such as furfural or camphor (Andreae and Merlet, 2001); 2) those impacted by anthropogenic emissions ($CO \geq 200$ ppb without the presence of furfural or camphor) and 3) those sampled in background conditions ($CO < 200$ ppb). Using the above criteria to distinguish between flights where we sampled fire plumes and those when we sampled background air we analysed the vertical profiles of species known to have a significant biomass burning source, such as NO_2, *ΣPNs*, *ΣANs*, *CO*, O_3 and some *VOCs* (i.e., propene, methacrolein, acetylene, benzene, ethyl-benzene, toluene, o-xylene, benzaldehyde, furfural and camphor). The CO and pyrogenic species analysis allows us to select five flights in which we distinguish between those where we sampled boreal fire emissions (B622, B623 and B624 – labelled henceforth "plume" flights) and those in which we measured background air (B619, B622 and B630 – labelled henceforth "background" flights). Flight B622 is a particular case in which both conditions are met, and we split this flight into two different parts: plume and background. Figure 3 shows profiles of the species indicated above as a function of the altitude for the plume flights (upper panels) and for the background flights (lower panels). It is possible to observe in Fig. 3 that the vertical structures are different in the two conditions. In the upper panels (plume flights) the concentrations of some species, especially *CO*, *ΣPNs*, Acetylene and Benzene, show significant and concomitant increases at 3500 m above sea level (a.s.l.) and 6000 m a.s.l.. Moreover, in the plume measurements at 2000 m a.s.l. a large increase in the CO levels is measured concurrent with an increase in the *ΣPNs*

smaller than at the other altitudes. This suggests that the conditions of the air masses at 2000 m a.s.l. are more complex and that it potentially has various origins, i.e., impacted both by anthropogenic and boreal biomass burning emissions. The *ΣANs* concentrations are lower than the *ΣPNs* and do not show significant structures. The O_3 profile shows little variability between 1000 and 7000 m of altitude with no concentration changes that coincide with variations in CO. In the background flights, as expected, the concentrations of the species analysed do not show strong vertical structures such as in the plume flights, with the exception of VOCs that show a peak at about 4 Km

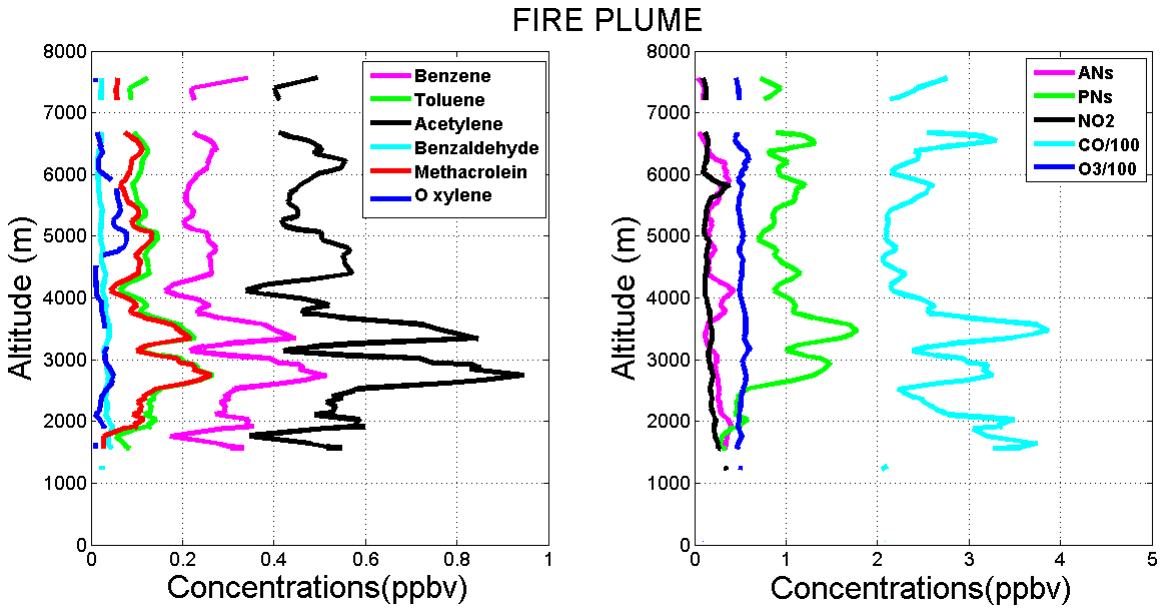

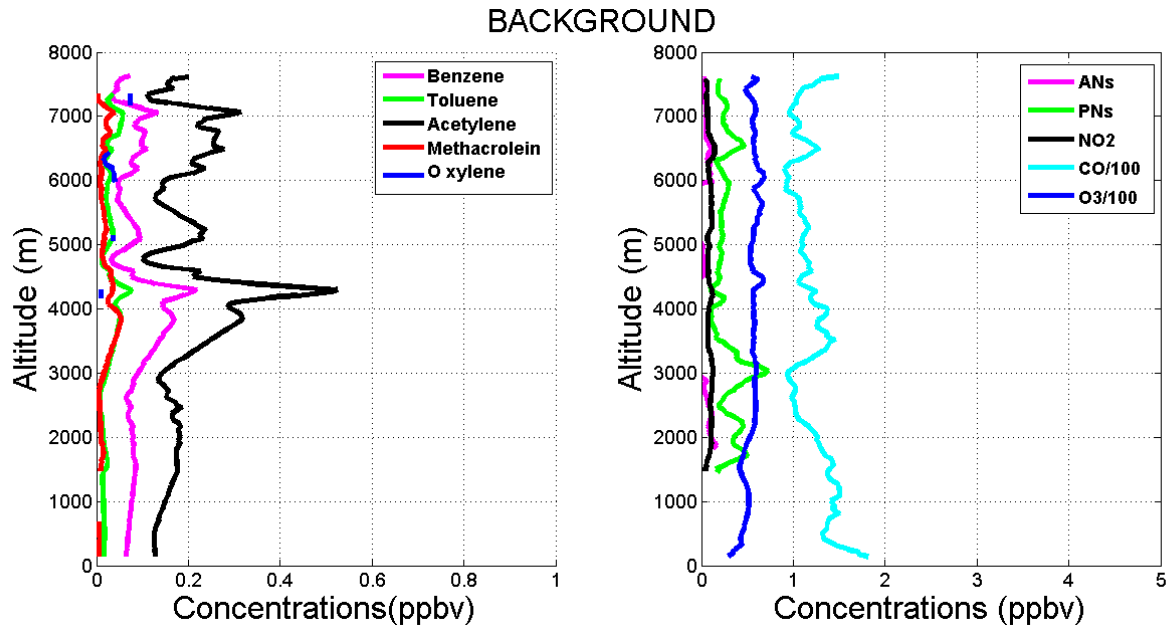

Figure 3. Vertical profiles of Benzene, Toluene, Acetylene, Methacrolein O-Xylene (panels on the left) and ΣANs, ΣPNs, NO_2, CO and O_3 (panels on the right) concentrations averaged for the plume flights (upper panels: B622, B623, B624 flights) and the background flights (lower panels: B619, B622, B630 flights).

To facilitate the determination of the sources of the biomass burning plumes (Tereszchuk et al., 2011; Parrington et al., 2012), we calculated Lagrangian back trajectories using the Hysplit model (Draxler et al., 2003) to verify the origin of the air masses. The Fire Locating And Monitoring of Burning Emissions (FLAMBE) archive provides fires emissions data from 2000 to the present worldwide (Reid et al., 2009) incorporating active fire detection data from geostationary and polar-orbiting satellites. To locate the sources of the boreal biomass burning plumes measured during the BORTAS campaign, the FLAMBE inventory data have been used in conjunction with the Hysplit back trajectories. In Fig. 4, 8 day back-trajectories are evaluated starting from points along the flight track and the corresponding fires (red asterisks) from the FLAMBE archive are shown for the plume flight B619 (upper panel) and for the background flight B623 (lower panel). The same analysis has been done for all the flights of the campaign, although here we report only the results of flights B619 and B623 since they are representative of all the other flights. Parrington et al. (2013) evaluated the photochemical age of the air masses for each flight using the ratio of *log(n-butane/ethane)* and assuming an *OH* concentration of 2×10^6 molecules/cm^3. They found that the age calculated for the air masses sampled within the boreal biomass burning emissions ranges between 1 and 5 days and the background air is older than 6 days.

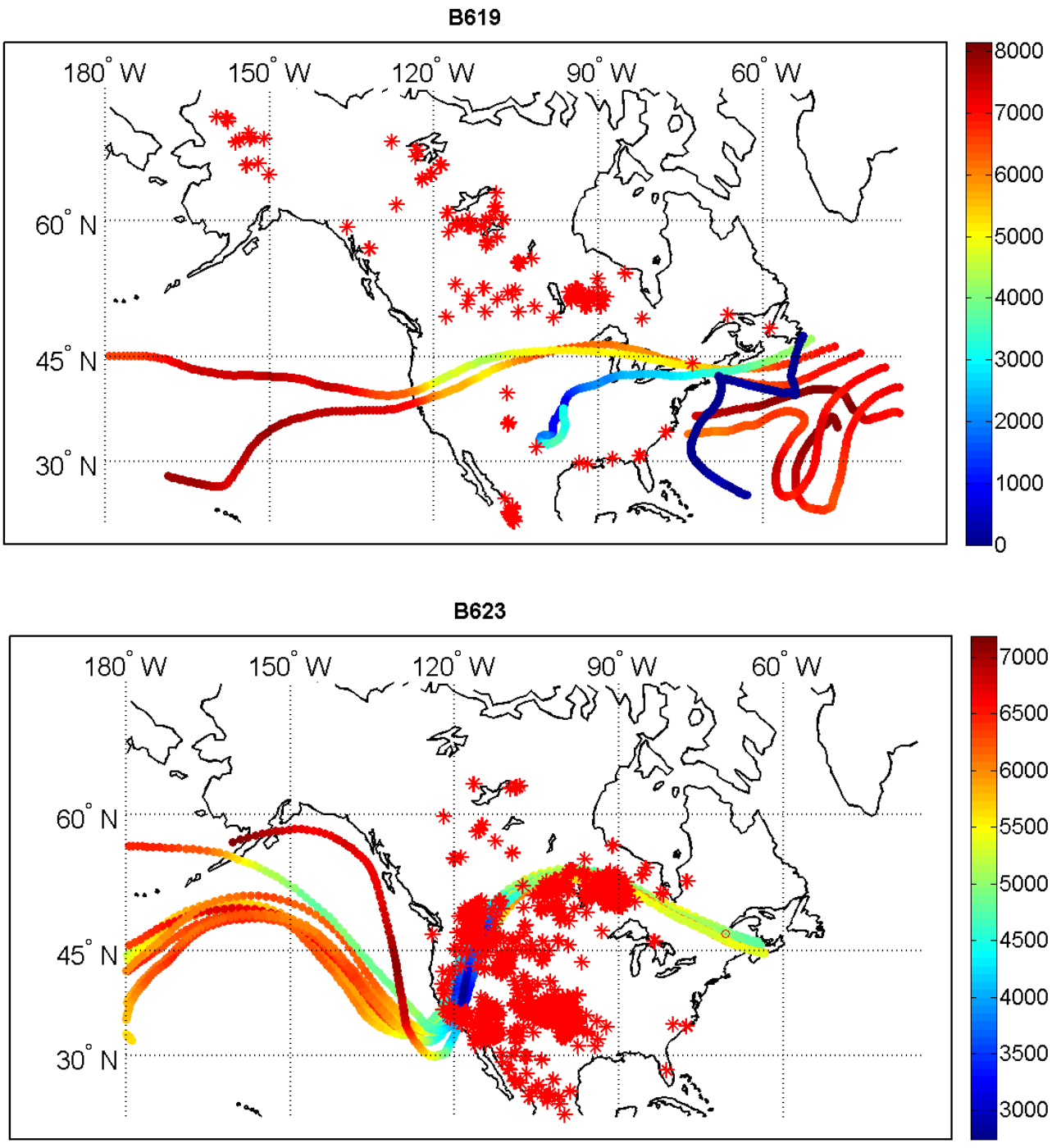

Figure 4. Location of the boreal biomass burning activity during the BORTAS campaign recorded by the FLAMBE inventory (red asterisks) and air mass backward trajectory analysis starting from location along the flight trajectories. The flight B623 (lower panel) sampled multiple fire plumes, whereas the flight B619 (upper panel) was representative of background conditions.

Their results are in agreement with the back-trajectories analysis, confirming that the air masses sampled during the plume flights crossed biomass fires during the previous 8 days and, conversely, the background air masses do not overlap fires up to 8 days before. In addition, Griffin et al.(2013) investigates boreal fire plumes during the BORTAS campaign using back trajectories calculated by the Canadian Meteorological Centre (CMC) and shows that the boreal fire plume originated from forest fires is approximately 1.5 days old, which is in agreement with the age calculated for the air masses sampled within the boreal biomass burning emissions.

3.3 Chemical signatures of plumes

In Figure 5 the time series of NO_2, ΣPNs, ΣANs, O_3, CO and furfural (when measured) for the B619 flight (top panel) and the B630 flight (bottom panel) are shown. During these background flights, the concentrations of all the species measured remain quite stable. The ΣPNs concentrations are significantly greater than the ΣANs but lower compared to those measured in the plume flights (less than 0.5 ppb). Moreover, ΣPNs do not show the significant structure that is shown in the O_3 measurements. CO is substantially lower than the 200 ppb threshold with the exception of one peak measured during B619 during a period spent in the airport for refueling (at ground level) where the CO level is affected by anthropogenic emissions and increases, reaching a maximum of about 300 ppb during take off.

The B622 flight shows two regimes, as indicated by the CO concentrations and by the furfural measurements. In the first part of the flight (between 2000 m a.s.l. and 4000 m a.s.l., highlighted by a grey box in Fig.5b) the CO levels (cyan line) exceed 150 ppb and the furfural (yellow line) shows three big plumes (up to 1.2 ppb) in which the ΣPNs also increase (reaching the maximum value of 3.5 ppb). On the other hand, in the second part of the flight the CO and ΣPNs decrease and the furfural is below the detection limit indicating that the air sampled is not affected by biomass burning. It is interesting to observe that O_3 and NO_2 concentrations are quite stable flying within or outside of the fire plume. Flight B623 (Fig. 5c) represents a case in which the air masses sampled

for most of the flight were impacted by biomass burning emissions and the remaining air masses show influence from human activities. In fact, CO levels are also always greater than 200 ppb and the furfural is below the detection limit during the whole flight, indicating an anthropogenic origin of the air masses. The fire plumes (highlighted by grey boxes) are characterized by sharp increases in the CO concentrations (maximum value of 552 ppb) and in the ΣPNs concentrations (maximum value of 1.5 ppb) measured while flying at constant altitude of about 4000 m a.s.l.. In the final part of flight B623 (between 00:26 and 01:00 UTC) a vertical spiral was carried out flying from 2000 m a.s.l. up to 8000 m a.s.l.. In this leg, plumes originating from different fires (identified analyzing the Hysplit back trajectories) were sampled. At about 4000 m a.s.l., back trajectories showed that the air masses sampled had the same origin of the fires plumes sampled at the same altitude in the first part of the flight. Both plumes were characterized by high levels of ΣPNs (up to 1.7 ppb). At the top of the spiral (8000 m a.s.l.), an aged plume was encountered with low ΣPNs and O_3 concentrations quite high (about 60 ppb). This high O_3 concentration represents the highest value measured during the whole flight.

According to the back-trajectories, this air mass originated from fires in the Western States of the U.S.A. (Oregon, Montana, Washington, Idaho, California, Nevada).

a)

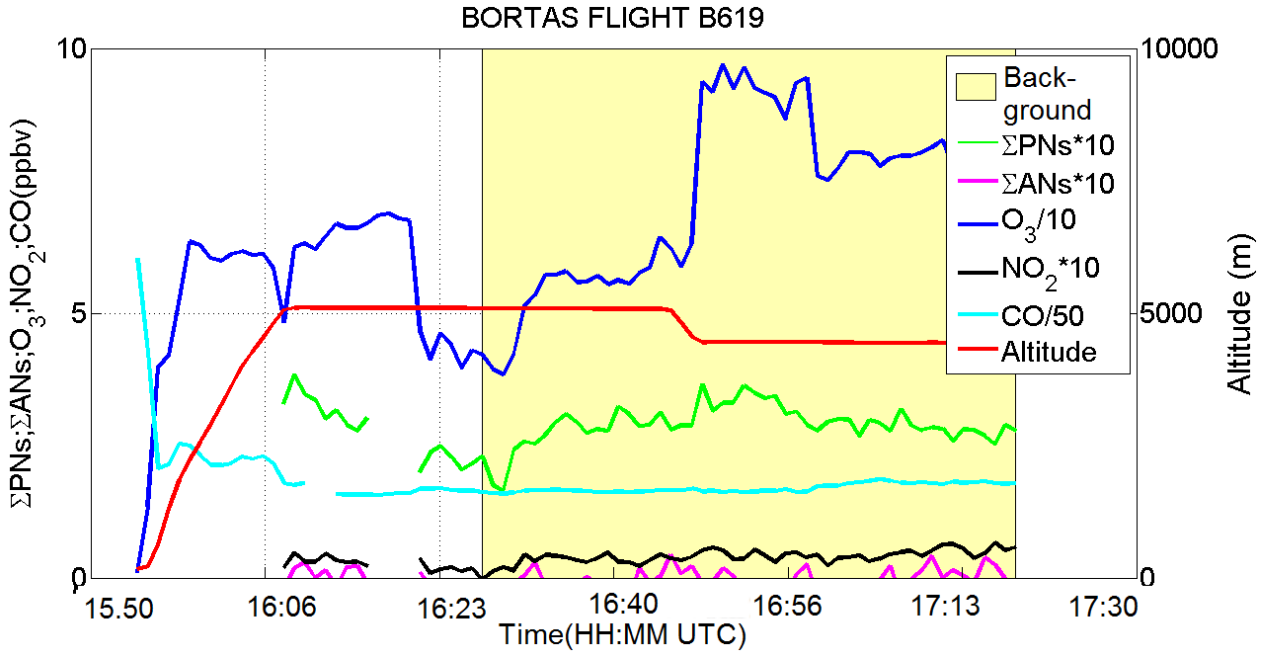
BORTAS FLIGHT B619
ΣPNs;ΣANs;O3;NO2;CO(ppbv)
Altitude (m)
Time(HH:MM UTC)
Back-ground
ΣPNs*10
ΣANs*10
O3/10
NO2*10
CO/50
Altitude
10
5
0
10000
5000
0
15.50
16:06
16:23
16:40
16:56
17:13
17:30

1
2

b)

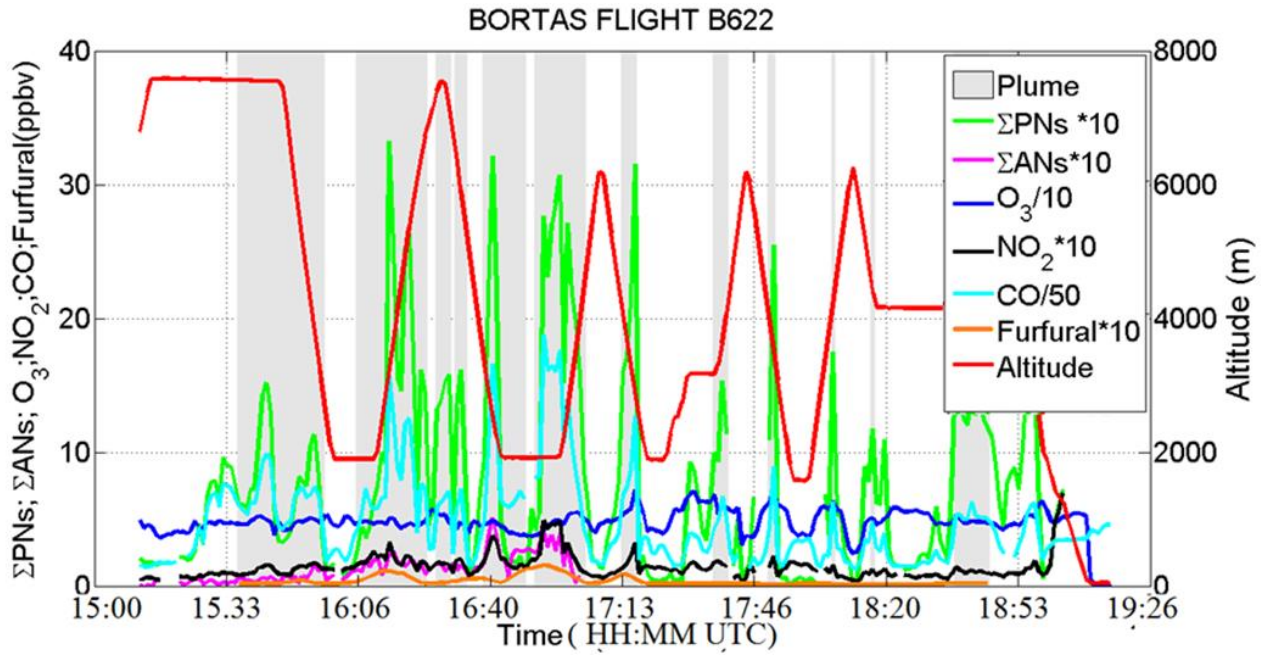
BORTAS FLIGHT B622
ΣPNs; ΣANs; O3;NO2;CO;Furfural(ppbv)
Altitude (m)
Time (HH:MM UTC)
Plume
ΣPNs *10
ΣANs*10
O3/10
NO2*10
CO/50
Furfural*10
Altitude
40
30
20
10
0
8000
6000
4000
2000
0
15:00
15.33
16:06
16:40
17:13
17:46
18:20
18:53
19:26

3
4

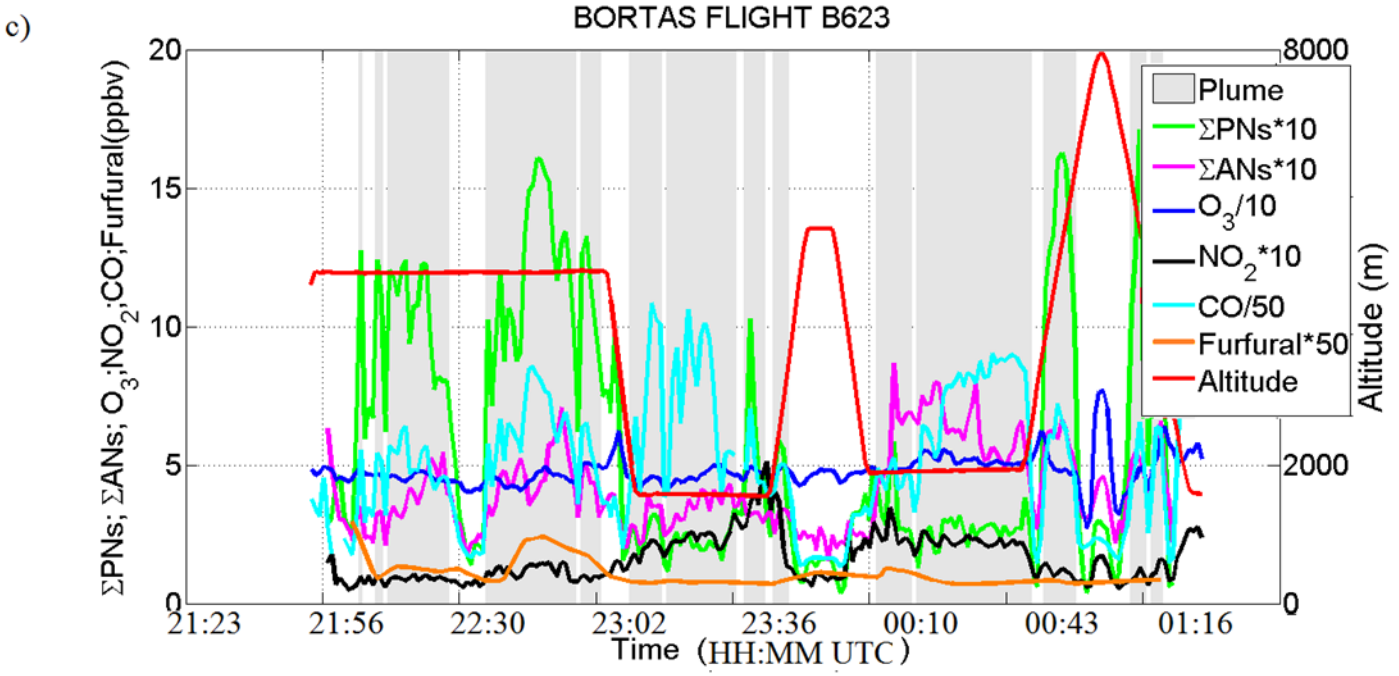

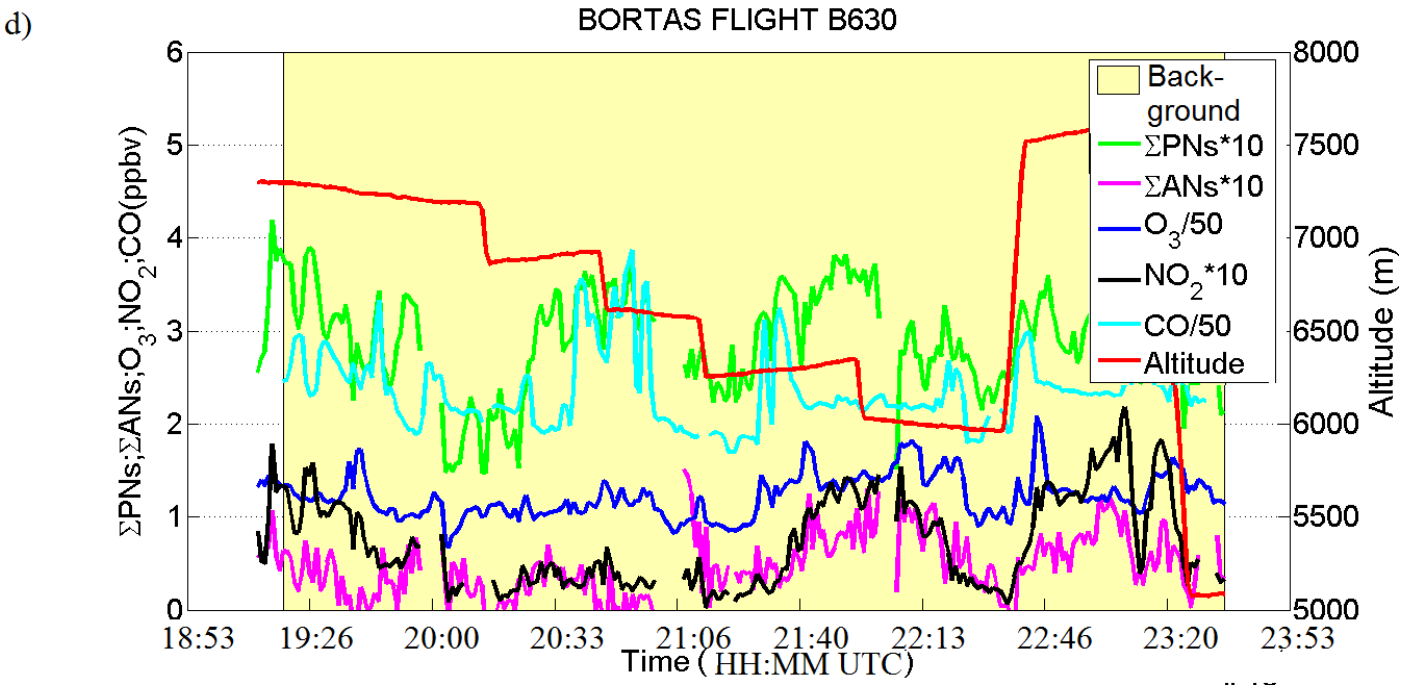

Figure 5. Time series of the ΣPNs, ΣANs, NO_2, O_3, CO, Furfural (ppbv) measured during the flights in this analysis: the flights B619 (panel a) and B630 (panel d) were background plumes , the flight B622 was in part impacted by fire plume and part by no-fire (panel b), the flight B623 (panel c) was affected by fire plume. The time is reported in Coordinated Universal Time (UTC).

3.4 ΣPNs and Ozone

The connection between O_3 and ΣPNs is highlighted by the scatterplot of ozone vs ΣPNs mixing ratios in Fig. 6. Two different dependences can be identified distinguishing the air masses that are representative of the background environment (flights B619, part of the B622 and B630) and those emitted or influenced by emissions from biomass burning (flights B623, B624 and part of B622). We distinguished between the "plume" and the "background" flights as described in Sect. 3.2: that ppb) and the pyrogenic species analysis. The linear fit of the data influenced by biomass burning emissions has a slope of ~1.87 ppb O_3/ppb ΣPNs compared to ~203.5 for the slope of the linear fit of background data, which indicates the important role played by the ΣPNs in the sequestration of ozone precursors in air masses influenced by fire emissions. This can be quantified by calculating the productions of O_3 and ΣPNs, following the ΣANs production schemes introduced by Atkinson (1985) and applied in other studies (Perring et al. 2010). Here we applied the same technique for the calculation of the PNs production defining the branching ratio for the peroxy nitrates as $\alpha = k_{R3}/(k_{R3}+k_{R4})$. Therefore, the net ΣPNs production is given by $\alpha(OH + RH + O_2 + NO_2 \rightarrow H_2O + RO_2NO_2)$ and the net O_3 production is described as $(1-\alpha)(RH + 4O_2 + h\nu \rightarrow H_2O + R'C(O) + 2O_3)$.

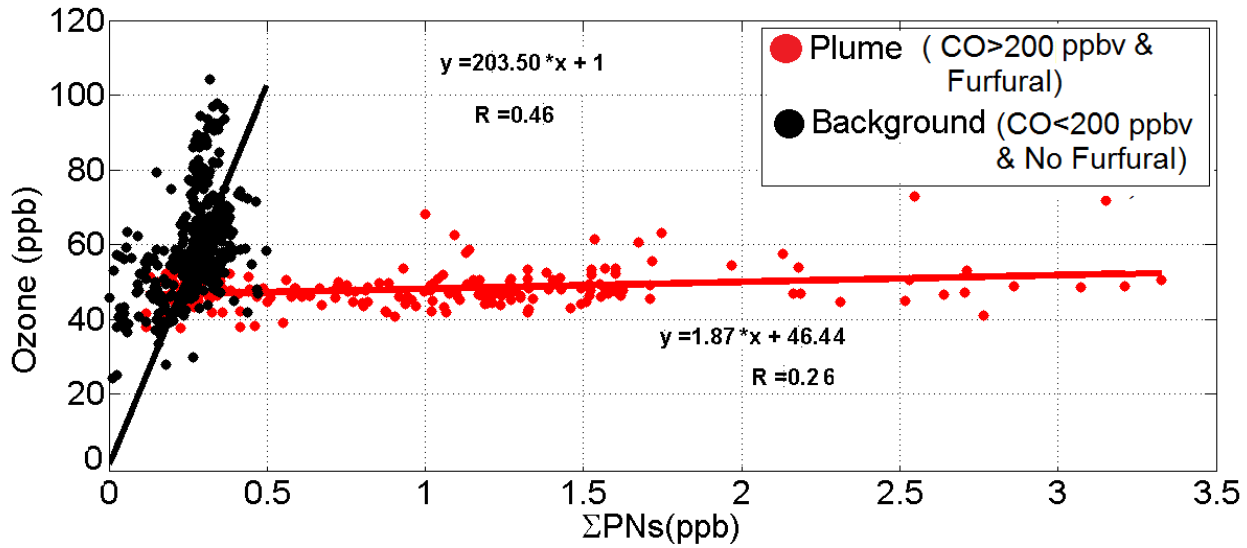

Figure 6. Scatter plot between measured O3 and measured ΣPNs for the flights B619, B622, B623, B624 and B630. Straight line is best fit linear regression. Plume identification follows the methodology and the analysis described in Sect. 3.2.

The production terms can be written as:

$$P\left(\sum PNs\right) = \sum_i \alpha_i k_{OH+RH_i}[OH][VOCs] \quad (1)$$

$$P(O_3) = \sum_i 2(1-\alpha_i) k_{OH+RH_i}[OH][VOC] + k_{OH+CO}[OH][CO] \quad (2)$$

where we considered the weighted sum of the contribution of each VOC to the ΣPNs and to the O_3 production. For the O_3 we take into account also the CO contribution on the $P(O_3)$ because of significant emissions associated with biomass burning.

In our analysis, we use two approaches to estimate the production of the ΣPNs and O_3: 1) a direct calculation considering the contribution to the PNs and O_3 production of all the VOCs, among those measured during BORTAS, that produce a PN species after first or second order reactions of the VOCs oxidation by OH; 2) a simulation using a box-model based on the Master Chemical Mechanism (MCM) where all the measured VOCs are used as input compounds to evaluate in output the production of PNs and O_3. The mechanism used to calculate directly the ΣPNs and O_3 production is similar for all the VOCs therefore we illustrate as an example the production mechanism of the perbenzoyl nitrate ($C_7H_5NO_5$), derived from the first-order oxidation of the benzaldehyde (C_7H_6O) (Figure 7, upper panel) and the production of the PN ($C_6H_5NO_7$), generated by the second-order oxidation of the benzene (Figure 7, lower panel). In the first case, abstraction of the aldehydic hydrogen by OH followed by O_2 addition forms an acyl peroxy radical ($C_7H_5O_3$). The acyl peroxy radical can react either with NO_2 forming the perbenzoyl nitrate or with NO producing $C_6H_5O_2$ and NO_2 (Figure 7, upper panel). In the second case, the production of PN starts with the benzene oxidation by OH forming three different products: 11.8% of these reactions generate

benzene-1,3,5-triol ($C_6H_6O_3$) and HO_2. The benzene-1,3,5-triol oxidation by OH, in turn, produces a molecule of $C_6H_5O_5$ in 31% of cases, that finally, reacts with NO_2 to form the peroxy nitrate $C_6H_5NO_7$ or with NO generating $C_5H_5O_4$ plus NO_2 (Figure 7, lower panel). For the branch of benzene oxidation that produces PN it is necessary to weight the contribution of the VOC oxidation to the PN formation by applying a branching ratio of 0.118 to the reaction constant for the initial benzene oxidation by OH and of 0.31 for the following benzene-1,3,5-triol oxidation: hereinafter we indicate the OH reaction constant weighted following this method as *k**. The same procedure has been applied also to the other VOCs that do not directly produce peroxy nitrates. Table 3 summarizes all the species involved in the evaluation of the ΣPNs and O_3 production during all the flights, indicating for each of them the OH reaction constant *k** and the branching ratio calculated as $\alpha = k_{R3}/(k_{R3} + k_{R4})$.

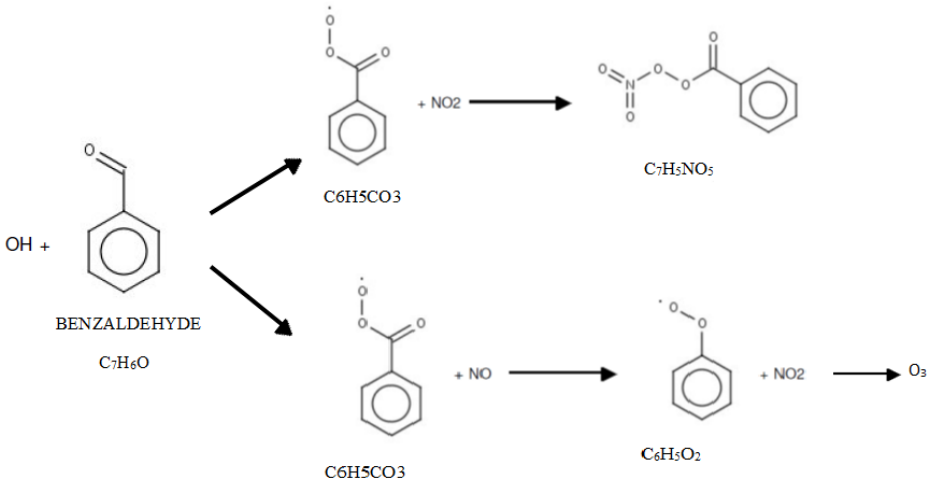

1

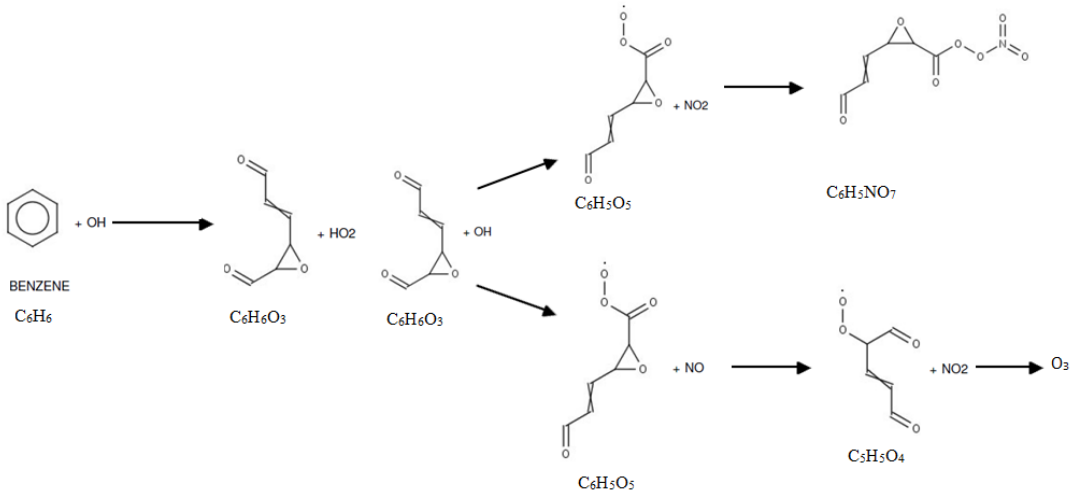

2

3 **Figure 7.** Examples of oxidation schemes that are common to all the VOCs that have as products
4 PNs and O_3. Upper panel: structural formula of the oxidation of benzaldehyde that produces directly
5 perbenzoyl nitrate ($C_7H_5NO_5$) and O_3. Lower panel: structural formula of the oxidation of benzene
6 that produce O_3 and indirectly the PN ($C_6H_5NO_7$).

7

8 **Table 3.** Species involved in the calculation of peroxy nitrate and ozone production, their weighted
9 reaction constant with OH (k* expressed in cm^3s^{-1}, see the text on how it is calculated) and the
10 ΣPNs branching ratio (α).

Species	k^*	α
Methacrolein	1.48×10^{-11}	0.2777
Acetylene	2.37×10^{-13}	0.3084
Benzene	4.16×10^{-14}	0.3084
Ethylbenzene	1.82×10^{-13}	0.3084
Toluene	1.97×10^{-13}	0.3084
O-Xylene	7.29×10^{-12}	0.3084
Benzaldehyde	1.36×10^{-11}	0.3084
CO	2.39×10^{-13}	0

The reaction constants were extracted from the MCM model data or the references therein, and from this, the branching ratios ($\alpha = k_{R3}/(k_{R3}+k_{R4})$) were calculated. For the branching ratio of Methacrolein, the value of k_{R4} is $(8.70\times10^{-12})\exp(290/T)$, where T is the temperature, and k_{R3} was evaluated following the MCM model procedure that takes into account the ambient pressure. For the other species, the k_{R4} reaction constant is $(7.50\times10^{-12})\exp(290/T)$, where T is the ambient temperature, and k_{R3} was evaluated as for methacrolein.

The simulation to retrieve the production of ΣPNs and O_3 were carried out using a 0-D Photochemical Box Model (UW Chemical Model, UWCM) that is based on the Master Chemical Mechanism (MCM) version v3.2 (http://mcm.leeds.ac.uk/MCM/) into a MATLAB-based source code (Wolfe and Thornton 2011). The MCM is a nearly-explicit reaction set including primary, secondary and radical species and about 17000 reactions to tracks all oxidation processes and products throughout the photochemical degradation of VOCs. The inorganic chemistry has been also included in the simulations. The photolysis reactions constants have been estimated from the TUV model (http://cprm.acd.ucar.edu/Models/TUV/). The model has been initialized using both the meteorological parameters (T, P, RH and J-values) and the chemical concentrations of NO, NO_2,

OH (fixed at 2 x 10^6 molecules/cm^3, as for the direct calculation), CO, O_3 and all the VOCs (see Table 4) measured during BORTAS campaign. As no OH measurements were made during the BORTAS campaign, its value was chosen to be representative of a northern mid-latitude summertime OH concentration (Spivakovsky et al., 2000). This assumption was validated by Parrington et al. (2013) carrying out several tests in order to compare the photochemical ages using different OH concentrations with the transport timescales from the emission source determined by back trajectory calculations. Table 4 summarizes the mean concentrations of the VOCs and other species used in the simulations, the ΣPNs and O_3 production and their ratio for each flight analysed. The species highlighted with one asterisk have been used also for the direct calculation of ΣPNs and O_3 production terms. The quantities highlighted with two asterisks are the production of PNs and O_3 calculated directly, while those without asterisks are the ΣPNs and O_3 production retrieved from the model simulations.

Table 4. Concentrations of each species involved in the ΣPNs and O_3 production (all reported in ppt), the production terms $P(O_3)$ and $P(\sum PNs)$ (expressed in ppt/s), their ratios $P(O_3)/P(\sum PNs)$ for all the flights analysed. While all the species reported in this table are used for the MCM model calculation of $P(O_3)$ and $P(\sum PNs)$, those with * are species used for the direct calculation of the production using the product between reaction constants and concentrations of the single species. The ΣPNs and O_3 production quantified with the model simulation are signed in this table with **. The selected flights are distinguished between the flights where we sampled boreal fire emissions (part of B622, B623 and B624 – labelled "plume" flights) and those in which we measured background air (B619, part of B622 and B630 – labelled "background" flights).

	Parameters	**B619**	**B622**	**B630**	**B622**	**B623**	**B624**
1	Ethane	1094.0	1209.8	975.1	4705.0	2407.5	1919.6
2	Propane	225.0	270.4	186.0	1141.2	563.4	432.3

3	n-Butane	42.9	53.7	36.9	258.7	133.4	89.8
4	i-Butane	16.8	17.9	18.6	73.3	36.7	33.8
5	n-Pentane	14.5	18.7	10.1	106.2	46.1	34.7
6	i-Pentane	9.6	16.7	5.6	37.6	19.3	47.7
7	n-Hexane	11.0	8.0	6.3	49.4	21.0	12.7
8	2+3-Methylpentane	5.0	6.6	39.4	19.4	7.5	10.4
9	n-Heptane	6.0	9.9	6.8	35.1	13.5	8.8
10	n-Octane	4.8	5.4	6.2	26.0	10.3	5.1
11	Ethene	419.0	585.4	67.2	5115.2	2038.4	452.5
12	Propene	27.1	27.4	10.1	1127.6	179.8	14.7
13	1-Butene	7.7	9.1	5.3	185.0	31.4	7.3
14	Trans-2-butene	4.0	4.3	4.5	3.3	4.8	6.1
15	i-Butene	6.0	6.1	6.8	84.1	12.2	6.5
16	1-Pentene	5.3	11.4	2.6	56.7	10.0	-
17	Trans-2-pentene	2.0	4.8	4.9	16.1	3.4	-
18	1,3-Butadiene	28.3	17.1	21.4	399.1	88.9	27.5
19	Isoprene	20.5	347.5	130.4	2796.3	763.0	231.0
20	Acetylene *	256.3	208.8	156.6	2053.6	887.8	480.4
21	Benzene *	115.5	81.1	51.6	1387.0	776.0	291.4
22	Toluene *	46.4	18.7	11.6	636.2	282.0	72.6
23	O-Xylene *	12.3	7.9	43.2	68.6	22.5	10.8
24	m+p-Xylene	33.6	20.6	36.0	117.8	42.8	12.2
25	E-Benzene *	19.9	13.1	35.3	90.6	97.6	19.9
26	Benzaldheyde *	-	26.0	-	68.0	30.5	88.6
27	Acetophenone	-	51.8	-	44.0	46.2	312.3
28	Acetone	1692.1	1959.9	2144.8	5561.7	3166.5	3594.0
29	Methyl vinyl ketone	-	319.7	-	4126.0	-	62.2

30	Methacrolein *	22.5	20.4	4.0	754.5	213.3	100.6
31	Methanol	2119.0	2731.7	1549.9	6369.9	3950.8	4677.3
32	Limonene	-	15.0	-	14.3	-	14.3
33	α-Pinene	-	29.1	-	18.5	17.5	19.3
34	Furfural	-	19.4	-	157.5	46.5	14.4
35	Camphor	-	18.5	-	26.2	15.5	15.3
36	NO_2	40.2	108.8	73.0	507.3	137.1	153.9
37	O_3	71824.8	48217	61195	42431.0	45425	50858
38	ΣPNs (ppt)	288.5	281.9	298.2	2981.2	1543.2	407.8
39	ΣANs (ppt)	148.9	72.3	46.9	404.8	399.8	335.0
40	CO (ppt)	84887.4	119559.0	119040	984590	419000	251540
	$P(O_3)$ (ppt/s) **	0.0420	0.0593	0.0581	0.5082	0.2120	0.1379
	$P(\sum PNs)$ (ppt/s)**	2.9719* 10^{-4}	4.6631* 10^{-4}	2.5807* 10^{-4}	0.0078	0.0023	0.0017
41	$P(O_3)/P(\sum PNs)$ **	141.3	127.2	225.0	65.0	90.3	78.9
	$P(O_3)$ (ppt/s)	0.5133	1.8446	0.5554	5.5643	0.6263	0.2432
	$P(\sum PNs)$ (ppt/s)	0.0035	0.0163	0.0053	0.1182	0.0341	0.0041
42	$P(O_3)/P(\sum PNs)$	145.6	113.5	105.4	47.1	18.3	58.8

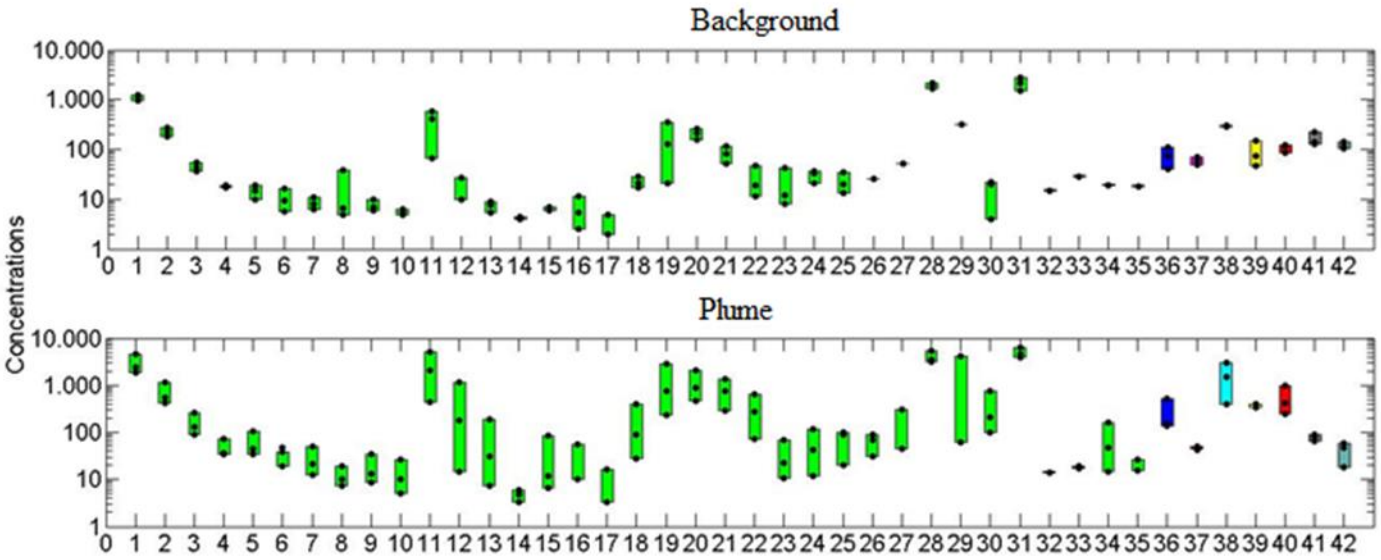

Figure 8. Average concentrations of the species involved in the O_3 and ΣPNs production. VOCs are in green, CO in red, NO_2 in blue, O_3 in magenta, ΣPNs in cyan and ΣANs in yellow. In grey is reported the ratio between the $P(O_3)$ and $P(\sum PNs)$ evaluated using the direct calculation (see section 3.3); in teal blue is reported the ratio between the $P(O_3)$ and $P(\sum PNs)$ evaluated using the model simulation. The upper shows data measured during background flights (B619, part of B622, B630); the lower panel shows data from fire plume flights (part of B622, B623, B624). The parameters showed in Figure 8 are numbered according to Table 4.

Figure 8 shows graphically the results summarized in Table 4. It is evident that during the background flights both the VOC (in green) and CO (in red) concentrations are significantly lower with respect to those measured during the plume flights, as expected. At the same time, however, the O_3 does not show significantly different concentrations in the biomass burning plumes. Conversely ΣPNs concentrations in the fire plumes increase to a level three times higher than the measurements in background air masses and the alkyl nitrates double. Analysing the measured concentrations of O_3 and ΣPNs, we deduced that the boreal biomass burning emissions affect the ΣPNs production more (on average 12 times higher in the fire plume compared with the background air) than the production, which increase by only 5 times in the fire plume. Using the MCM

simulation we got a slightly different increase of ΣPNs production in the fire plume (on average 7 times), whereas the O_3 production in the fire plume on average increases 2 times. Therefore in the fire plumes sampled during the BORTAS campaign, with both methods we observed more production of NO_x reservoir species, which can be transported and potentially impact the O_3 concentrations in other locations. Alvarado et al. (2010), using a global chemical-transport model, estimated that 40% of the initial NO_x emission from boreal forest fires were converted into PAN. Since PAN is one of the compounds included in ΣPNs family, our results show that more production of ΣPNs in fire plumes compared with background air is plausible. Moreover, calculating the ozone and peroxy nitrate production ratio (Fig. 6), we found that it is lower in the fires plumes than in the background samples. This suggests that the production of peroxy nitrates during the boreal biomass burning becomes a significant process compared with the ozone production, at least in cold air when the thermal dissociation of ΣPNs is not efficient. For example PAN, which is usually the most abundant ΣPNs, has a lifetime strongly dependent on temperature: 1 hr at 300 K, 2 days at 273 K and 118 days at 250 K (Isaksen, 1985). In order to understand the impact of a specific category of VOCs, we calculated the contribution of each VOC species and CO on the ΣPNs and O_3 production for the fire plume flights (B622, B623 and B624). We find that the ozone production, as expected, is dominated by CO (with percentages exceeding 93% for all the flights). Moreover, the production of peroxy nitrates is dominated by methacrolein (with percentages ranging between 38% and 86%), followed by benzaldehyde (47%-7%) and o-xylene (19%-3%). An unusual case, in terms of the peroxy nitrates production, is the background flight (B630) during which 75% of $P(\sum PNs)$ is derived from o-xylene and only 13% from methacrolein, which dominates on all the other flights analysed in this study. At first look this is strange because methacrolein is one of the major products of isoprene oxidation and it is expected that air masses coming from boreal forests (burning or not) would be characterized by high concentrations of biogenic VOCs rather than o-xylene which is an anthropogenic VOC. Lai et al.

(2013) found that at the Taipei International Airport (Taiwan) the most abundant VOCs produced by the aircraft exhaust emissions is o-xylene. During the B630 flight the altitude was of about 7000 m a.s.l. (ranging between 7500-6000 m.a.s.l.), higher than the other flights (1700-6000 m.a.s.l.), and the flight track was around the eastern coast of Canada: Nova Scotia and Newfoundland Island. At the flight altitude of B630 it is possible to sample air masses affected by aircraft emissions and, so it is likely that the o-xylene dominance on the ΣPNs production can be explained due to emissions from aircraft traffic.

Finally, the analysis of the O_3 and ΣPNs production in different environments (background and boreal biomass burning plumes) indicates the impact on the tropospheric O_3 budget of the fire emissions. In fact, the air masses influenced by biomass burning emissions show a lower (about 90 with the direct method and about 40 with the model) $P(O_3)/P(\sum PNs)$ ratio with respect to that for the background air masses (about 180 with the direct method and about 120 with the model) suggesting that the ozone production in the fire plumes is less significant than the peroxy nitrate formation, on the contrary of what occurs in the background air masses. The difference between the calculate ratios and the measured O_3/ΣPNs (see Fig. 6) can be explained considering that: 1) the air masses are not fresh emissions; 2) the ΣPNs production (term at the denominator) is underestimated, as expected since we are not considering all the possible VOCs precursors but only the available for the BORTAS campaign. Moreover, the higher VOCs and ΣPNs concentrations measured during the fire plume flights, associated with stable O_3 levels in the two environments, are indicative of processed air masses (produced 4-5 days before) and suggest that NO_2 reservoir species are produced in these plumes and transported to other regions.

4. Conclusions

In July and August 2011 the BORTAS aircraft campaign was carried out in Canada investigating the impact of the emissions of boreal biomass burning on tropospheric chemistry. We analysed the ΣPNs and O_3 production in two different environments (air masses affected by fire emissions and those representative of background air) and using different approaches: 1) a direct calculation in which we considered the VOCs oxidation rate constant and the ΣPNs branching ratios for all the VOCs species that produce PN after the first or second order reaction of their oxidation by OH; 2) using a 0-D photochemical model based on MCM that includes a detailed chemistry of all the VOCs measured. Comparing the production of ΣPNs and O_3 in plumes impacted by fire emissions with that in background air, we found that, on average, ΣPNs production is more strongly enhanced than O_3 production: 5 - 12 times versus 2 - 7 times. Boreal biomass burning plumes observed during BORTAS campaign show minimal enhancement of the O_3 and NO_2 concentrations and slight enhancement of the O_3 production. However, they show significant enhancement in both concentration and production of ΣPNs, which can act as a reservoir and enhance ozone production downwind of the plume.

Acknowledgments

The BORTAS project was supported by the Natural Environment Research Council (NERC) under grant number NE/F017391/1. M. Parrington was supported by the NERC grant. P. I. Palmer acknowledges support from his Philip Leverhulme Prize.

References

Alvarado, M. J., J. A. Logan, J. Mao, E. Apel, D. Riemer, D. R. Blake, R. C. Cohen, K.-E. Min, A. Perring, E. C. Browne, P. J. Wooldridge, G. S. Diskin, G. Sachse, H. Fuelberg, W. R. Sessions, D. L. Harrigan, L. G. Huey, J. Liao, A. Case-Hanks, J. Jimenez-Palacios, M. J. Cubison, S. A. Vay, A. Weinheimer, D. J. Knapp, D. D. Montzka, F. Flocke, I. B. Pollack, P. Wennberg, A. Kurten, J. D. Crounse, J. M. St. Clair, A. Wisthaler, T. Mikoviny, R. M. Yantosca, C. C. Carouge, and P. Le Sager :Nitrogen oxides and PAN in plumes from boreal fires during

ARCTAS-B and their impact on ozone: an integrated analysis of aircraft and satellite observations, Atmos. Chem. Phys., 10, 9739-9760, doi:10.5194/acp-10-9739-2010,2010.

Amiro, B. D.,Cantin, A., Flannigan, M. D. and De Groot, W. J.: Future emissions from Canadian boreal forest fires, Canadian Journal of Forest Research, 39(2), 383–395, doi:10.1139/X08-154, 2009.

Andreae, M. O. and Merlet, P.: Emission of trace gases and aerosols from biomass burning, Global Biogeochem. Cy., 15, 955–966, 2001.

Atkinson, R., Kinetics and Mechanisms of the Gas-Phase Reactions of the Hydroxyl Radical with Organic Compounds under Atmospheric Conditionsm Chem. Rev. 85, 89-201, 1985.

Bowman, DMJS, J.K. Balch, P. Artaxo, W.J. Bond, J.M. Carlson, M.A. Cochrane, C.M. D'Antonio, R.S. DeFries, J.C. Doyle, S.P. Harrison, F.H. Johnston, J.E. Keeley, M.A. Krawchuk, C.A. Kull, J.B.Marston, M.A. Moritz, I.C. Prentice, C.I. Roos, A.C. Scott, T.W. Swetnam, G.R. van der Werf, and S.J. Pyne: Fire in the earth system, Science, 324, 481-484, 2009.

Chan, C. Y., Chan, L. Y., Harris, J. M., Oltmans, S. J., Blake, D. R., Qin, Y., Zheng, Y. G., and Zheng, X. D.: Characteristics of biomass burning emission sources, transport, and chemical speciation in enhanced springtime tropospheric ozone profile over Hong Kong, J. Geophys. Res., 108, 4015, doi:10.1029/2001JD001555, 2003.

Chia-Hsiang Lai, Kuen-Yuan Chuang, Jin-Wei Chang: Source Apportionment of Volatile Organic Compounds at an International Airport, Aerosol and Air Quality Research, 13: 689–698, 2013 Copyright © Taiwan Association for Aerosol Research ISSN: 1680-8584 print / 2071-1409 online doi: 10.4209/aaqr.2012.05.0121

Crutzen, P.J., L.E. Heidt, J.P. Krasnec, W.H. Pollock and W. Seiler: Biomass burning as a source of atmospheric gases CO, H_2 , N_2O, NO, CH_3Cl and COS. Nature , 282 , 253-256, 1979.

Dari-Salisburgo, C., Carlo, P. D., Giammaria, F., Kajii, Y., and D'Altorio, A.: Laser induced fluorescence instrument for NO2 measurements: Observations at a central Italy background site,Atmos. Environ., 43, 970–977, 2008.

Day, D. A., P. J. Wooldridge, M. B. Dillon, J. A. Thornton, and R. C. Cohen: A thermal dissociation laser-induced fluorescence instrument for in-situ detection of NO2, peroxy nitrates, alkyl nitrates, and HNO3, J. Geophys. Res.,107(D6), 4046, doi:10.1029/2001JD000779,2002.

Di Carlo, P., Aruffo, E., Busilacchio, M., Giammaria, F., Dari-Salisburgo, C., Biancofiore, F., Visconti, G., Lee, J., Moller, S., Reeves, C. E., Bauguitte, S., Forster, G., Jones, R. L., and Ouyang, B.: Aircraft based four-channel thermal dissociation laser induced fluorescence instrument for simultaneous measurements of NO2, total peroxy nitrate, total alkyl nitrate, and HNO3, Atmos. Meas. Tech., 6, 971–980, doi:10.5194/amt-6-971-2013,2013.

Draxler, R. R.: HYSPLIT4 user's guide, Tech. Rep. NOAA Tech. Memo. ERL ARL-230, NOAA Air Resources Laboratory, Silver Spring, MD, 1999.

Gerbig, C., S. Schmitgen, D. Kley, A. Volz-Thomas, K. Dewey, and D. Haaks: An improved fast-response vacuum-UVresonance fluorescence CO instrument, J. Geophys. Res.,104 (D1), 1699–1704, 1999.

Gillett, N., A. J. Weaver, F. W. Zwiers, and M. D. Flannigan : Detecting the effect of climate change on Canadian forest fires, Geophys.Res. Lett., 31, L18211, doi:10.1029/2004GL020876,2004.

Goode, J. G., Yokelson, R. J., Ward, D. E., Susott, R. A., Babbitt, R. E., Davies, M. A., and Hao, W. M.: Measurements of Excess O_3, CO_2, CO, CH4, C2H4, C2H2, HCN, NO, NH3, HCOOH, CH3COOH, HCHO and CH3OH in 1997 Alaskan Biomass Burning Plumes by Airborne Fourier Transform Infrared Spectroscopy (AFTIR), J. Geophys. Res., 105, 22147–22166, 2000.

Griffin D., Walker K. A., Franklin J. E. , Parrington M., Whaley C. , Hopper J., Drummond J. R.,Palmer P. I. , Strong K., Duck T. J. , Abboud I., Bernath P. F., Clerbaux C. , Coheur P.F. , Curry K. R. ,Dan L. ,Hyer E. , Kliever J. , Lesins G., Maurice M., Saha A. , Tereszchuk K., and Weaver D. Investigation of CO, C2H6 and aerosols in a boreal fire plume over eastern Canada during BORTAS 2011 using ground- and satellite-based observations and model simulations Atmos. Chem. Phys., 13, 10227–10241, 2013

Hopkins, J. R., Read, K. A., and Lewis, A. C.: Two column method for long-term monitoring of non-methane hydrocarbons (NMHCs) and oxygenated volatile organic compounds, J. Environ.Monitor., 5, 8–13, 2003.

Jacob, D. J., Wofsy, S. C., Bakwin, P. S., Fan, S.-M., Harriss, R.C., Talbot, R.W., Bradshaw, J., Sandholm, S., Singh, H. B., Gregory,G. L., Browell, E. V., Sachse, G. W., Blake, D. R., and Fitzjarrald, D. R.: Summertime photochemistry at high northern latitudes, J. Geophys. Res., 97, 16421–16431, 1992.

Jaffe, D.A.,Wigder,N.L.: Ozone production from wildfires: A critical review. Atmospheric Environment 51, 1–10, doi:10.1016/j.atmosenv.2011.11.063,2012.

Jenkin, M. E., Saunders, S. M., Wagner, V., and Pilling, M. J.: Protocol for the development of the Master Chemical Mechanism, MCM v3 (Part B): tropospheric degradation of aromatic volatile organic compounds, Atmos. Chem. Phys., 3, 181–193, doi:10.5194/acp-3-181-2003, 2003.

Isaksen, I. S. A., ed., Tropospheric Ozone: Regional and Global Scale Interactions, D. Reidel Pub. Co., Dordrecht, NATO ASI Series C, Vol. 227, 1988.

Langmann, B., Duncan, B., Textor, C., Trentmann, J., and van der Werf, G. R.: Vegetation fire emissions and their impact on air pollution and climate, Atmos. Environ., 43, 107–116, 2009.

Lapina, K., Honrath, R.E., Owen, R.C., Val Martın, M., and Pfister, G.: Evidence of significant large–scale impacts of boreal fires on ozone levels in the midlatitude Northern Hemisphere free troposphere. Geophys. Res. Lett. 33, L10815, 2006.

Lavoué D, Liousse C, Cachier H, Stocks BJ, Goldammer JG. :Modeling of carbonaceous particles emitted by boreal and temperate wildfires at northern latitudes. J. Geophys. Res.: Atmos. 105(D22): 26871-26890,2000.

Lee, J. D., Moller, D. J., Read, K. A., Lewis, A. C., Mendes, L., and Carpenter, L. J.: Year-round measurements of nitrogen oxides and ozone in the tropical North Atlantic marine boundary layer, J.Geophys. Res., 114, D21302, doi:10.1029/2009JD011878, 2009.

Leung, F.-Y. T., Logan, J. A., Park, R., Hyer, E., Kasischke, E., Streets, D., and Yurganov, L.: Impacts of enhanced biomass burning in the boreal forests in 1998 on tropospheric chemistry and the sensitivity of model results to the injection height of emissions, J. Geophys. Res., 112, D10313, doi:10.1029/2006JD008132, 2007.

Lewis, A. C., Evans, M. J., Hopkins, J. R., Punjabi, S., Read, K.A., Purvis, R. M., Andrews, S. J., Moller, S. J., Carpenter, L.J., Lee, J. D., Rickard, A. R., Palmer, P. I., and Parrington, M.:The influence of biomass burning on the global distribution of selected non-methane organic compounds, Atmos. Chem. Phys., 13, 851–867, doi:10.5194/acp-13-851-2013, 2013.

Marlon, J. R., Bartlein, P. J., Carcaillet, C., Gavin, D. G., Harrison, S. P., Higuera, P. E., Joos, F.,Power, M. J., and Prentice, I. C.: Climate and human influences on global biomass burning over the past two millennia, Nature Geoscience , 1, 69–702, 2008.

Mauzerall, D., Jacob, D. J., Fan, S.-M., Bradshaw, J., Gregory, G., Sachse, G., and Blake, D.: Origin of tropospheric ozone at remote high northern latitudes in summer, J. Geophys. Res., 101, 4175–4188, 1996.

Murphy, J. G., Oram, D. E., and Reeves, C. E.: Measurements of volatile organic compounds over West Africa, Atmos. Chem. Phys., 10, 5281–5294, doi: 10.5194/acp-10-5281-2010 , 2010.

Nault, B. A., Garland, C., Pusede, S. E., Wooldridge, P. J., Ullmann, K., Hall, S. R., Cohen, and R. C.: Measurements of CH3O2NO2 in the upper troposphere, Atmos. Meas. Tech., 8, 987–997, 2015.

Palmer, P. I., Parrington, M., Lee, J. D., Lewis, A. C., Rickard, A.R., Bernath, P. F., Duck, T. J., Waugh, D. L., Tarasick, D. W.,Andrews, S., Aruffo, E., Bailey, L. J., Barrett, E., Bauguitte, S. J.-B., Curry, K. R., Di Carlo, P., Chisholm, L., Dan, L., Forster, G., Franklin, J. E., Gibson, M. D., Griffin, D., Helmig, D., Hopkins, J. R., Hopper, J. T., Jenkin, M. E., Kindred, D., Kliever, J.,Le Breton, M., Matthiesen, S., Maurice, M., Moller, S., Moore,D. P., Oram, D. E., O'Shea, S. J., Owen, R. C., Pagniello, C.M. L. S., Pawson, S., Percival, C. J., Pierce, J. R., Punjabi,

S.,Purvis, R. M., Remedios, J. J., Rotermund, K. M., Sakamoto,K. M., da Silva, A. M., Strawbridge, K. B., Strong, K., Taylor,J., Trigwell, R., Tereszchuk, K. A., Walker, K. A., Weaver, D.,Whaley, C., and Young, J. C.: Quantifying the impact of BOReal forest fires on Tropospheric oxidants over the Atlantic using Aircraft and Satellites (BORTAS) experiment: design, execution and science overview, Atmos. Chem. Phys., 13, 6239–6261, doi:10.5194/acp-13-6239-2013, 2013.

Parrington, M., Palmer, P. I., Henze, D. K., Tarasick, D. W., Hyer, E. J., Owen, R. C., Helmig, D., Clerbaux, C., Bowman, K. W.,Deeter, M. N., Barratt, E. M., Coheur, P.-F., Hurtmans, D., Jiang, Z., George, M., and Worden, J. R.: The influence of boreal biomass burning emissions on the distribution of tropospheric ozone over North America and the North Atlantic during 2010,Atmos. Chem. Phys., 12, 2077–2098, doi:10.5194/acp-12-2077- 2012, 2012.

Parrington, M., Palmer, P. I., Lewis, A. C., Lee, J. D., Rickard, A. R., Di Carlo, P., Taylor, J. W., Hopkins, J. R., Punjabi, S., Oram, D. E., Forster, G., Aruffo, E., Moller, S. J., Bauguitte, S. J.-B., Allan, J. D., Coe, H., and Leigh, R. J.: Ozone photochemistry in boreal biomass burning plumes, Atmos. Chem. Phys., 13, 7321–7341, doi:10.5194/acp-13-7321-2013, 2013.

Pfister, G., Emmons, L. K., Hess, P. G., Honrath, R., Lamarque, J.-F., Val Martin, M., Owen, R. C., Avery, M., Browell, E. V., Holloway J. S., Nedelec, P., Purvis, R., Rywerson, T. B., Sachse,G.W., and Schlager, H.: Ozone production from the 2004 North American boreal fires, J. Geophys. Res., 111, D24S07, doi:10.1029/2006JD007 695, 2006.

Perring A.E., Bertram T.H., Farmer D.K., Wooldridge P.J., Dibb J., Blake N.J., Blake D.R., Singh H.B., Fuelberg H., Diskin G., Sachse G., and Cohen R.C. The production and persistence of ∑RONO2 in the Mexico City plume, Atmos. Chem. Phys., 10, 7215–7229, 2010.

Purvis, R. M., Lews, A. C., Hopkins, J. R., Andrews, S., and Minaean, J.: Functionalized aromatic compounds within middle troposphere boreal biomass burning plumes, in preparation, 2013.

Real, E., Law, K. S., Weinzierl, B., Fiebig, M., Petzold, A., Wild, O., Methven, J., Arnold, S., Stohl, A., Huntrieser, H., Roiger,A., Schlager, H., Stewart, D., Avery, M., Sachse, G., Browell, E., Ferrare, R., and Blake, D.: Processes influencing ozone levels in Alaskan forest fire plumes during long-range transport over the North Atlantic, J. Geophys. Res., 112, D10S41,doi:10.1029/2006JD007576, 2007.

Reid, J. S., Hyer, E. J., Prins, E. M., Westphal, D. L., Zhang, J.,Wang, J., Christopher, S. A., Curtis, C. A., Schmidt, C. C., Eleuterio,D. P., Richardson, K. A., and Hoffman, J. P.: Global monitoring and forecasting of biomass burning smoke: Description of and lessons from the Fire Locating and Modeling of Burning Emissions (FLAMBE) program, IEEE J. Sel. Top. Appl., 2,144–162, 2009.

Reidmiller, D. R., Jaffe, D. A., Fischer, E. V., and Finley, B.: Nitrogen oxides in the boundary layer and free troposphere at the Mt. Bachelor Observatory, Atmos. Chem. Phys., 10, 6043–6062,doi:10.5194/acp-10-6043-2010, 2010.

Rinsland, C. P., Dufour, G., Boone, C. D., Bernath, P. F., Chiou, L. Coheur, P.-F., Turquety, S., and Clerbaux, C. :Satellite boreal measurements over Alaska and Canada during June–July 2004: Simultaneous measurements of upper tropospheric CO, C_2H_6, HCN, CH_3Cl, CH_4,C_2H_2, CH_3OH, HCOOH, OCS, and SF6 mixing ratios, Global Biogeochemical Cycles, Vol.21, GB3008,doi:10.1029/2006GB002795, 2007.

Saunders, S. M., Jenkin, M. E., Derwent, R. G., and Pilling, M. J.:WWW site of a master chemical mechanism (MCM) for use in tropospheric chemistry models, Atmos. Environ., (Report Summary), 31, 1249, 1997.

Saunders, S. M., Jenkin, M. E., Derwent, R. G., and Pilling, M. J.: Protocol for the development of the Master Chemical Mechanism, MCM v3 (Part A): tropospheric degradation of nonaromatic volatile organic compounds, Atmos. Chem. Phys., 3, 161–180, doi:10.5194/acp-3-161-2003, 2003.

Simpson, I. J., Rowland, F. S., Meinardi, S., and Blake, D. R. :Influence of biomass burning during recent fluctuations in the slow growth of global tropospheric methane, Geophys. Res. Lett., 33, L22808,doi:10.1029/2006GL027330, 2006.

Spivakovsky, C. M., Logan, J. A., Montzka, S. A., Balkanski, Y. J., Foreman-Fowler, M., Jones, D. B. A., Horowitz, L. W., Fusco, A. C., Brenninkmeijer, C. A. M., Prather, M. J.,Wofsy, S. C., and McElroy, M. B.: Three-dimensional climatological distribution of tropospheric OH: Update and evaluation, J. Geophys. Res., 105, 8931–8980, 2000.

Tereszchuk, K. A., Gonz´alez Abad, G., Clerbaux, C., Hurtmans, D., Coheur, P.-F., and Bernath, P. F.: ACE-FTS measurements of trace species in the characterization of biomass burning plumes,Atmos. Chem. Phys., 11, 12169–12179, doi:10.5194/acp-11-12169-2011, 2011.

Val Martin, M., Honrath, R., Owen, R. C., Pfister, G., Fialho, P., and Barata, F.: Significant enhancements of nitrogen oxides, ozone and aerosol black carbon in the North Atlantic lower free troposphere resulting from North American boreal wildfires, J. Geo-phys. Res., 111, D23S60, doi:10.1029/2006JD007530, 2006.

Verma, S., Worden, J., Pierce, B., Jones, DBA., Al-Saadi, J., Boersma, F., Bowman, K., Eldering, A., Fisher, B., Jourdain, L., Kulawik, S., Worden, H. :Ozone production in boreal fire smoke plumes using observations from the Tropospheric Emission Spectrometer and the Ozone Monitoring Instrument, J. Geophys. Res., 114, 0.1029/2008JD010108,2009.

Wilson, K. L. and J. W. Birks: Mechanism and Elimination of a Water Vapor Interference in the Measurement of Ozone by UV Absorbance, Environmental Science and Technology 40, 6361-6367,2006.

Wofsy, S.C., Sachse, G.W., Gregory, G.L., Blake, D.R., Bradshaw, J.D., Sandholm, S.T., Singh, H.B., Barrick, J.A., Harriss, R.C., Talbot, R.W., Shipham, M.A., Browell, E.V., Jacob, D.J. and Logan, J.A.:Atmospheric chemistry in the Arctic and subarctic: Influence of natural fires, industrial emissions, and stratospheric inputs. Journal of Geophysical Research 97: doi: 10.1029/92JD00622. issn: 0148-0227, 1992.

Wolfe, G.M. and Thornton, J.A.: The Chemistry of Atmosphere Forest Exchange (CAFE) Model - Part 1:Model Description and Characterization, Atmospheric Chemistry and Physics, 11, 77-101, 2011.

Wotawa, G., and M. Trainer :The influence of Canadian forest fires on pollutant concentrations in the United States. Science 288(5464):324-328,2000.

Wotton, B. M., Nock, C. A., and Flannigan, M. D.: Forest fire occurrence and climate change in Canada, International Journal of Wildland Fire, 19, 253–271, 2010.